

# Ion energy distributions in inductively coupled radio-frequency discharges in argon, nitrogen, oxygen, chlorine, and their mixtures

Yicheng Wang<sup>a)</sup> and J. K. Olthoff<sup>b)</sup>

Electricity Division, Electronics and Electrical Engineering Laboratory, National Institute of Standards and Technology, Gaithersburg, Maryland 20899-8113

(Received 12 November 1998; accepted for publication 21 January 1999)

We report ion energy distributions, relative ion intensities, and absolute total ion current densities at the grounded electrode of an inductively coupled Gaseous Electronics Conference radio-frequency reference cell for discharges generated in pure argon, nitrogen, oxygen, and chlorine, and in mixtures of argon with  $N_2$ ,  $O_2$ , and  $Cl_2$ . Measured current densities are significantly greater for pure argon and for mixtures containing argon than for pure  $N_2$ ,  $O_2$ , and  $Cl_2$ . For all three molecular gases, the ratio of molecular ions to the fragment ions decreases when argon is added to the molecular gas discharges. A possible destruction mechanism for the molecular ions involving metastable argon is discussed. © 1999 American Institute of Physics. [S0021-8979(99)00309-6]

## I. INTRODUCTION

Ion bombardment plays a key role in the plasma etching of semiconductor materials, and therefore determination of the identity, flux, and energies of the ions striking the surfaces exposed to etching plasmas has attracted much interest.<sup>1</sup> However, most of the investigations of ions in processing plasmas have been applied to capacitively coupled reactors, and only recently have investigations been extended to high density plasmas generated in inductively coupled reactors.<sup>2-7</sup>

In this article we present mass analyzed ion-energy distributions (IEDs) and ion flux densities measured by a combined ion energy analyzer-mass spectrometer that sampled plasma ions through an orifice in the lower electrode of an inductively coupled Gaseous Electronics Conference (GEC) radio-frequency (rf) reactor. Data are presented for plasmas generated in pure argon, nitrogen, oxygen, and chlorine, and in mixtures of argon containing 20%  $N_2$ ,  $O_2$ , or  $Cl_2$  by volume. It is shown for high density plasmas containing these molecular gases, that mass analysis of the ion flux is essential since the identities of the dominant ions are dependent upon the plasma parameters. This is unlike many low density capacitively coupled plasmas where the dominant ion is nearly always the molecular ion.<sup>8</sup>

The GEC rf reference reactor concept was developed to facilitate the comparison of experimental plasma data between different laboratories, and to help clarify the effect of reactor design on plasma conditions. Earlier measurements of ion-energy distributions have been made by researchers at Sandia National Laboratories for argon, chlorine, and argon: chlorine plasmas in an inductively coupled GEC rf reference reactor using a retarding potential analyzer.<sup>5-7</sup> The results presented here are in reasonable agreement with these previously published results in pure argon, but some significant differences in measured ion energies and relative ion flux

densities are observed in chlorine-containing plasmas that are attributed to subtle differences in the GEC reactors used in the different laboratories.

## II. EXPERIMENT

### A. GEC rf reference reactor

Plasmas were generated in a GEC rf reference reactor<sup>9,10</sup> whose upper electrode was modified to house a five-turn planar rf-induction coil behind a quartz window to produce inductively coupled discharges.<sup>11</sup> The reactor, along with the ion-energy analyzer and mass spectrometer, are shown schematically in Fig. 1. The feed gas entered the cell through one of the 2 3/4 in. side flanges and was pumped out through the 6 in. port attached to the turbo-molecular pump. The gas pressure was maintained by a variable gate valve between the pump and the GEC cell. The flow was maintained by mass flow controllers at 7.45  $\mu\text{mol/s}$  (10 sccm) for all of the experiments reported here.

The discharge was generated by applying a 13.56 MHz voltage to the coil in the upper electrode through a matching network. The rf power values presented in this article are the net power to the matching network driving the coil. The actual rf power dissipated in the plasma has been determined to be approximately 80% of the powers listed.<sup>11</sup> The lower electrode was grounded to the vacuum chamber.

Ions were sampled through a 10  $\mu\text{m}$  diam orifice in a 2.5  $\mu\text{m}$  thick nickel foil that was spot welded into a small counter bore in the center of the stainless steel lower electrode. The lower electrode used here was similar to the modified electrode assembly used in our previous investigations of ion-energy distributions in a capacitively coupled GEC rf reactor.<sup>12</sup> For "standard" inductively coupled GEC cells,<sup>11</sup> the lower electrode is covered by a 0.32 cm (1/8 in.) thick stainless steel plate that extends the diameter of the lower electrode to 16.5 cm (6.5 in.). This is obviously not possible for these experiments since it is necessary to sample ions through a hole in the lower electrode. Therefore, the lower electrode used here was further modified to allow the place-

<sup>a)</sup>Electronic mail: yicheng.wang@nist.gov

<sup>b)</sup>Electronic mail: james.olthoff@nist.gov

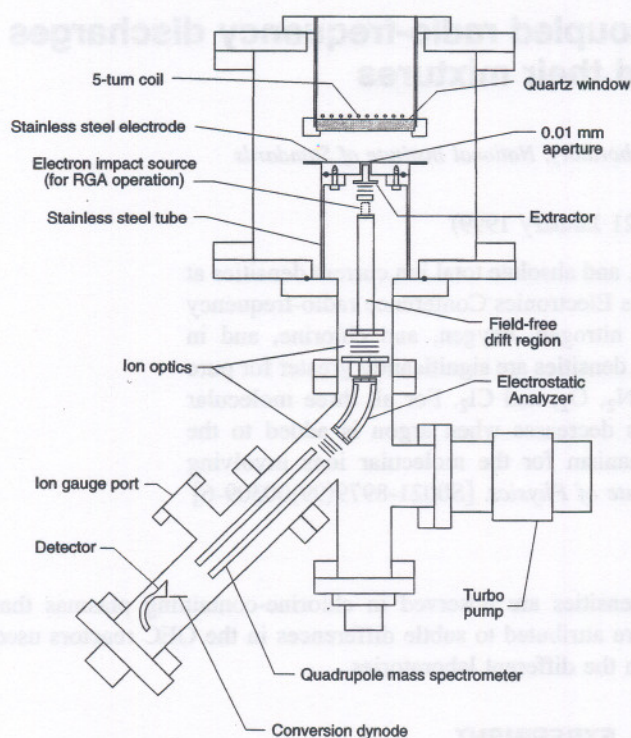


FIG. 1. Schematic diagram of the inductively coupled GEC rf reference reactor with the ion-energy analyzer and mass spectrometer appended to the modified lower electrode.

ment of a flat, 0.32 cm thick, stainless steel ring around the outer edge of the electrode that extended the effective electrode diameter from 10.2 to 16.5 cm without covering the center of the lower electrode. The spacing from the surface of the quartz window in the top electrode to the surface of the lower grounded electrode was 4.13 cm. The lower electrode was not water cooled, so care was taken not to run the plasmas at high power for extended periods of time.

### B. Ion energy and mass analyzers

The mass spectrometer with ion-energy analyzer used here is the same instrument used to measure ion-energy distributions in a capacitively coupled GEC rf reactor,<sup>12</sup> and in high pressure dc Townsend discharges.<sup>13</sup> Briefly, ions are sampled through the 10  $\mu\text{m}$  diam orifice in the center of the grounded electrode. For IED measurements, the ions that pass through the orifice are accelerated and focused into a 45° electrostatic energy selector. After being selected according to their energy, the ions enter a quadrupole rf mass filter where they are also selected according to their mass-to-charge ratio ( $m/z$ ). The system is operated so that ions always pass through the energy and mass selectors with the same kinetic energy regardless of their initial energy upon entering the sampling orifice. The energy resolution of the selector was fixed at a value of  $\Delta\epsilon=1$  eV, full width at half maximum (FWHM). A channeltron electron multiplier with associated pulse counting electronics served as the ion detector of the mass filter. The recorded IEDs correspond to fluxes (ion counts per second) recorded for ions incident on the grounded electrode surface with fixed  $m/z$  at different ener-

gies. At each nominal energy,  $\epsilon$ , the recorded flux corresponds to ions with energies in the range between  $\epsilon-\Delta\epsilon/2$  and  $\epsilon+\Delta\epsilon/2$  determined by the energy resolution of the instrument. The ion flux recording times were the same for all energies, and the uncertainty in the energy scale is estimated to be  $\pm 1.0$  eV.

Past experience with the ion-energy analyzer<sup>13</sup> indicates that the ion transmission is uniform over the ion-energy ranges observed here when tuned properly. The mass dependence of the transmission of the quadrupole mass spectrometer was determined in two ways. First, by comparing the electron-impact mass spectrum taken of sulfur hexafluoride ( $\text{SF}_6$ ) with a standard mass spectrum of this gas.<sup>14</sup> This is a convenient way of determining the mass transmission since  $\text{SF}_6$  has equally spaced peaks over a mass range from 32 to 127 u. Second, ion-energy distributions were measured for ions sampled from different rare gas plasmas (Ne, Ar, Kr, and Xe) at the appropriate power settings such that the total ion current was constant in each case. A plot of the ion mass versus the mass spectrometer response provides the transmission curve (one must account for the isotopes of the rare gases). Both methods produced analogous curves that showed that the mass transmission was uniform up to 40 u. For ions with mass greater than 40 u (only  $\text{Cl}_2^+$  for the gases studied here) the absolute measured intensities were adjusted as prescribed by the transmission curve.

For total ion current measurements (i.e., all ion current passing through the sampling orifice), the ion optic elements at the front of the ion-energy analyzer were biased such that all of the current passing through the sampling orifice was collected on the extractor element (the first ion optic element behind the electrode surface; see Fig. 1). The total current collected on the extractor element was measured with an electrometer. The magnitude of the measured current went to zero when the plasma was off, thus indicating that the source of the measured current is ions being sampled from the plasma. The absolute intensities of the IEDs were scaled to the measured values of the total ion current. The ion flux densities presented here were derived by dividing the total measured ion current by the area of the 10  $\mu\text{m}$  diam sampling hole.

## III. RESULTS AND DISCUSSION

### A. Argon

The total ion flux densities measured in the present experiments for argon discharges at 100 and 300 W and pressures ranging from 0.34 to 6.67 Pa (2.5 to 50 mTorr) are shown in Fig. 2 (solid symbols). These data indicate increasing ion current with increasing gas pressure for both power levels, in agreement with previous measurements.<sup>5</sup> The error bars for our data represent a single standard deviation calculated from eight measurements made over the course of several weeks, and indicate that the measurements are reproducible to within approximately  $\pm 10\%$ .

Previous measurements of the current density as a function of pressure by Woodworth *et al.*<sup>5</sup> are shown by the open symbols in Fig. 2. Our data shown in Fig. 2 exhibit pressure and power dependencies that agree with the previous mea-

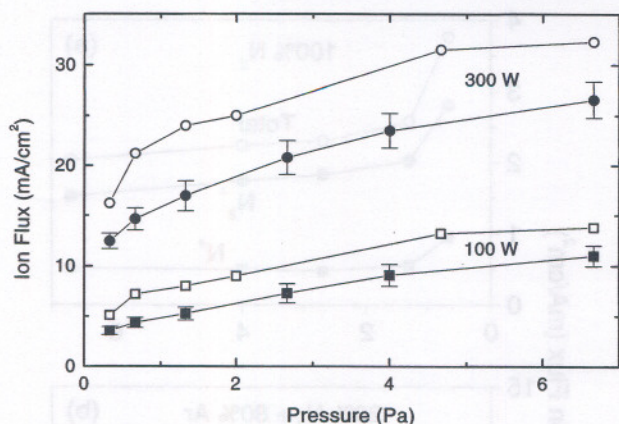


FIG. 2. Measured total ion flux densities for inductively coupled argon plasmas as a function of gas pressures at 300 and 100 W. The solid symbols are the data obtained from the present experiments, and the open symbols are previously published data of Woodworth *et al.* (see Ref. 5), also obtained on a GEC rf reference cell.

measurements, but the magnitude of the ion flux densities measured here are as much as 30% below those measured by Woodworth *et al.*<sup>5</sup> There are many possible reasons for these differences including: (1) different electrode spacings due to differences in the way the stainless steel plate was added to the lower electrode; (2) minor differences in the coil geometry and position due to inconsistencies in the fabrication process; (3) different power coupling efficiencies; (4) temperature effects due to the use of an uncooled lower electrode in the present experiment; (5) unquantified changes in the surface conditions of the electrodes due to sputtering and deposition; (6) differences in the radial distributions of the ion flux density that affect the density at the center of the electrode; (7) uncertainties in pressure measurements; and (8) general uncertainties from extrapolating a flux density from an ion current measured through a small orifice.

Using the same GEC cell as utilized in these experiments, Sobolewski<sup>15</sup> measured the dc ion saturation current at the lower electrode, and obtained an ion flux density of 13 mA/cm<sup>2</sup> for an argon plasma at 1.33 Pa and 350 W. This value is in general agreement with both our and Woodworth's measurements at 300 W when one takes into account the nonuniformity of the discharge across the electrodes (Sobolewski's measurements are an average current density for the entire electrode) and the different powers used. In general, considering the possible differences between the different GEC cells, agreement within 30% can be considered reasonable. In fact, initial measurements of electrical parameters made on capacitively coupled GEC cells to determine reproducibility exhibited similar levels of agreement.<sup>9</sup>

Figure 3 shows the measured ion-energy distributions for Ar<sup>+</sup> ions sampled from argon plasmas for pressures ranging from 0.34 to 6.7 Pa and powers of 100 and 300 W. The magnitude of each of the IEDs has been normalized to the total ion currents shown in Fig. 2. Ar<sup>+</sup> is the dominant ion in the argon plasmas studied here, with Ar<sup>++</sup> accounting for less than 2% of the ion signal and no Ar<sub>2</sub><sup>+</sup> being detected. The ion-energy distributions in Fig. 3 exhibit the relatively narrow shape observed previously for ions sampled from in-

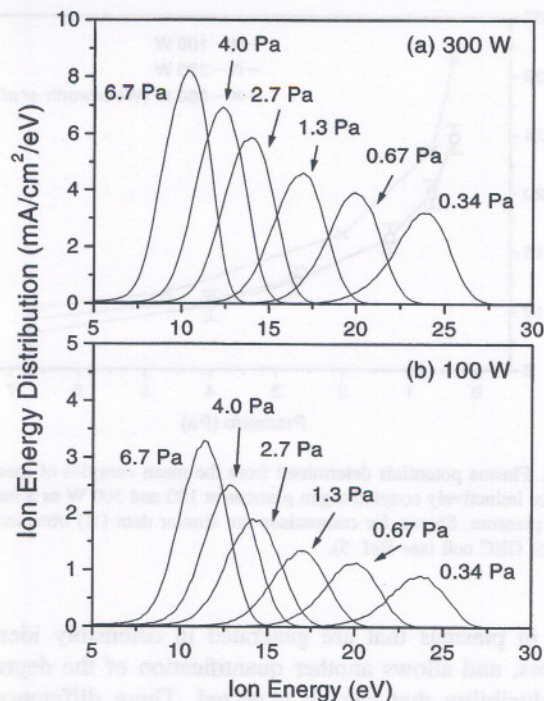


FIG. 3. Kinetic energy distributions of Ar<sup>+</sup> ions from an inductively coupled argon plasma at the pressures indicated and for applied rf powers of (a) 300 W and (b) 100 W. Ions were sampled at the lower, grounded electrode of a modified GEC rf reference cell.

ductively coupled plasmas,<sup>5</sup> similar to IEDs measured from capacitively coupled plasmas under collisionless sheath conditions.<sup>12</sup> The mean ion energy decreases with increasing pressure, but the FWHM is nearly constant as the pressure and power are varied. The FWHM measured here is approximately 3.1 eV, which is slightly greater than the 2.8 eV observed by Woodworth *et al.*<sup>5</sup> on their GEC cell, and indicates a larger degree of capacitive coupling between the coil and the plasma in our reactor. As was evident in Fig. 2, the ion flux densities are significantly lower for the 100 W discharge than for the 300 W discharge.

The mean energies of the IEDs in Fig. 3 correspond to the plasma potential ( $V_p$ ) of the inductively coupled discharge. Figure 4 shows a plot of the plasma potentials, derived from the measured IEDs, as a function of pressure for 100 and 300 W plasmas. As was previously observed,<sup>5</sup> the plasma potential is nearly independent of power, indicating that for the plasmas studied here the input power controls the electron density but not the mean energy of the electrons. However, the plasma potential is highly dependent upon gas pressure with  $V_p$  decreasing with increasing pressure. This decrease can be attributed to a decrease in the electron energies as the pressure increases. The plasma potentials at 300 W measured by Woodworth *et al.*<sup>5</sup> (shown for comparison in Fig. 4) exhibit the same general pressure dependence, but are somewhat higher in magnitude than those measured here, particularly at the lower pressures. Measurements of the plasma potentials in argon plasmas performed previously on our GEC cell,<sup>16</sup> using a Langmuir probe, are 1–2 eV higher than those measured by Woodworth. These apparent inconsistencies again illustrate the potential for plasma varia-

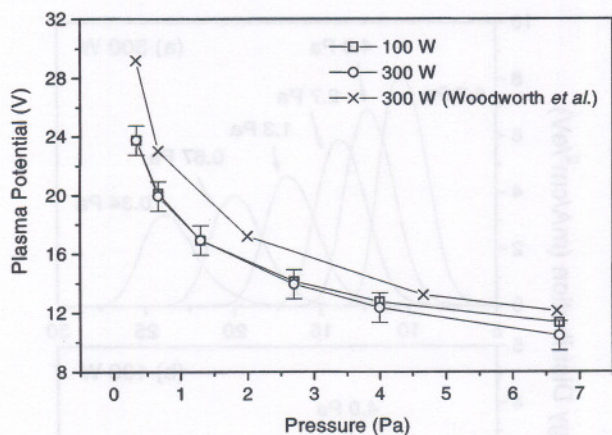


FIG. 4. Plasma potentials determined from the mean energies of measured IEDs for inductively coupled argon plasmas at 100 and 300 W as a function of gas pressure. Shown for comparison are similar data ( $\times$ ) obtained on a different GEC cell (see Ref. 5).

tions in plasmas that are generated in ostensibly identical reactors, and allows another quantification of the degree of reproducibility that can be expected. These differences in plasma potentials can be attributed to many of the causes listed above for the differences observed in ion flux densities, but the most likely causes are differences in surface conditions (such as surface charging, differing secondary electron and photoemitted electron yields, and changes in work functions).

## B. Nitrogen and Ar:N<sub>2</sub> mixtures

Figure 5(a) shows the ion flux densities at the grounded electrode for 300 W inductively coupled plasmas generated in pure nitrogen for pressures ranging from 0.34 to 6.7 Pa (2.5 to 50 mTorr). The open symbols represent the total ion flux density measured using the technique described in Sec. II B. The total ion flux is significantly lower in pure N<sub>2</sub> than in argon at all pressures, by more than a factor of 10 at the highest pressures. This corresponds to comparably lower electron densities observed in N<sub>2</sub> plasmas compared to those measured in argon plasmas.<sup>16</sup> In further contrast to the argon data, the ion flux density for N<sub>2</sub> plasmas decreases with increasing pressure.

The solid symbols in Fig. 5(a) represent the relative contributions of the N<sub>2</sub><sup>+</sup> and N<sup>+</sup> ions to the total ion flux density. The N<sub>2</sub><sup>+</sup> ion is the dominant ion at all pressures, with N<sup>+</sup> accounting for 20%–25% of the total ion flux. While the N<sub>2</sub><sup>+</sup> flux dominates the total ion signal, the relative magnitude of the N<sup>+</sup> flux compared to the N<sub>2</sub><sup>+</sup> flux with the inductively coupled plasma source is significantly greater than that observed in capacitively coupled GEC cells.<sup>8</sup> Additionally, unlike for capacitively coupled plasmas, no N<sub>3</sub><sup>+</sup> or N<sub>4</sub><sup>+</sup> ions were observed here, presumably due to the lower gas pressures and correspondingly lower probability of three-body collisions in the inductively coupled plasmas.

Figure 5(b) shows the total ion flux for an inductively coupled plasma sustained in a 20% N<sub>2</sub>:80% Ar mixture at 300 W as a function of gas pressure. The total flux density is observed to be significantly greater in the mixture, closer to

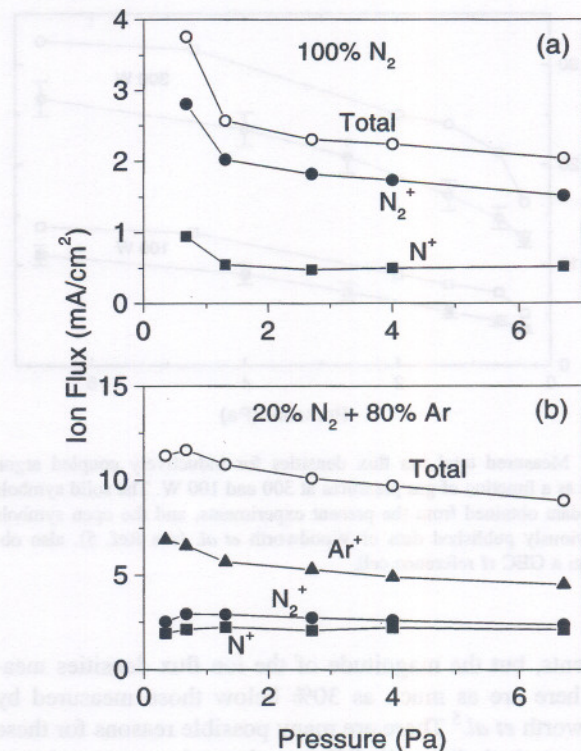


FIG. 5. Absolute ion flux densities at the grounded electrode for 300 W inductively coupled plasmas in (a) pure N<sub>2</sub> and in (b) a mixture (by volume) of 20% N<sub>2</sub> with argon. The open symbols ( $\circ$ ) are the total ion flux densities derived from the total current measurements. The closed symbols are determined from the relative intensities of the measured IEDs for each ion scaled to the total flux densities: ( $\bullet$ ) N<sub>2</sub><sup>+</sup>, ( $\blacksquare$ ) N<sup>+</sup>, and ( $\blacktriangle$ ) Ar<sup>+</sup>.

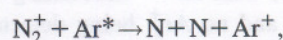
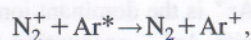
the densities observed in pure argon than in pure nitrogen. However, the magnitude of the total ion flux exhibits a downward trend as the pressure increases, contrary to that observed in pure Ar but similar to that observed in pure N<sub>2</sub>.

The dominant ion detected from the argon–nitrogen mixture is Ar<sup>+</sup>. The nitrogen ions exhibit significant, but smaller, intensities. Interestingly, the measured intensities of the N<sub>2</sub><sup>+</sup> and N<sup>+</sup> ions are nearly equal for the mixture, in sharp contrast to the relative intensities of these ions in pure nitrogen. The decrease of N<sub>2</sub><sup>+</sup> ion flux relative to N<sup>+</sup> may be due, in part, to the presence of argon metastable species (Ar\*) in the discharge. Ar\*(3<sup>3</sup>P<sub>2</sub>) has a static polarizability<sup>17</sup> of 323 a<sub>0</sub><sup>3</sup> (nearly 30 times that of ground state Ar),<sup>18</sup> and thus would be expected to have a strong long-range interaction probability with N<sub>2</sub><sup>+</sup> and N<sup>+</sup>. The corresponding Langevin orbiting rate coefficients would be equal to 4 × 10<sup>-9</sup> and 5 × 10<sup>-9</sup> cm<sup>3</sup>/s, respectively, for N<sub>2</sub><sup>+</sup> and N<sup>+</sup>.

For N<sup>+</sup> reacting with Ar\*, the charge transfer process,



is the only available reaction. For N<sub>2</sub><sup>+</sup>, several energetically allowed reactions are possible



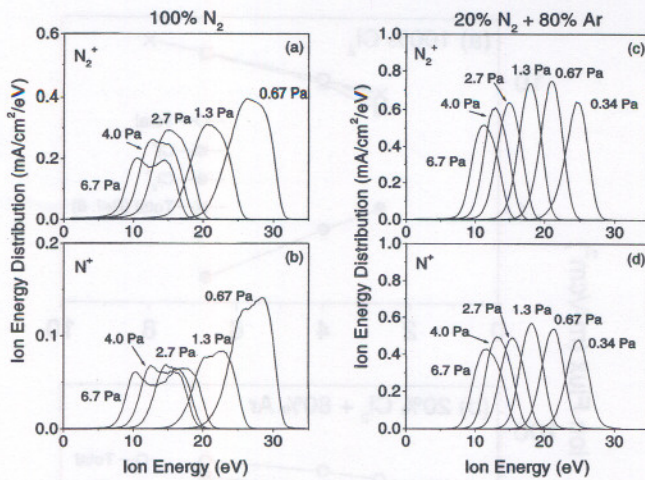


FIG. 6. Ion-energy distributions for  $N_2^+$  and  $N^+$  sampled from 300 W inductively coupled plasmas in pure  $N_2$  [(a) and (b)] and in a mixture of 20%  $N_2$  in argon [(c) and (d)] for the pressures indicated.

each of which destroys a  $N_2^+$  ion, and one of which generates a  $N^+$  ion. The energetics of these reactions allows them to take place within the glow of the discharge, and the multiple reaction pathways for interactions of  $N_2^+$  with  $Ar^*$  may lead to an efficient destruction mechanism for  $N_2^+$ . No information on the cross sections or branching ratios of these interactions is presently available.

Interactions between metastable argon and  $N_2$  molecules are also possible, with the only energetically possible reaction resulting in the dissociation of  $N_2$  into two N atoms. However, this process is not expected to play a significant role in the plasmas studied here since earlier measurements indicate that the degree of dissociation of nitrogen in similar  $N_2:Ar$  plasmas is small.<sup>19</sup> Penning ionization is not energetically allowed.

The ion-energy distributions for  $N_2^+$  and  $N^+$  from pure  $N_2$  are shown in Figs. 6(a) and 6(b), respectively. The IEDs for  $N_2^+$  and  $N^+$  are similar in shape, and as expected, exhibit nearly the same mean energies. The IEDs in the pure nitrogen discharge are significantly broader (FWHM=6.8 eV) than the IEDs for  $Ar^+$  in pure argon, and exhibit a barely resolved "saddle structure" or splitting. In a capacitively coupled discharge, this splitting would be indicative of thinner sheaths in nitrogen than in argon, but in fact the opposite is true. The lower ion currents measured in nitrogen, compared to argon, indicate that the plasma density is lower, which implies larger sheaths in nitrogen. The larger sheaths result in a greater capacitive voltage drop across the ground sheath which broadens the ion energy distribution in nitrogen compared to argon. The saddle structure is more pronounced in the IEDs for  $N^+$  than for  $N_2^+$ , due to the shorter transit time across the sheath for  $N^+$  resulting from its lighter mass. The mean energies of the nitrogen IEDs are approximately 2 eV higher than those measured for argon, indicating correspondingly larger plasma potentials and higher electron temperatures.<sup>16</sup>

The ion-energy distributions for  $N_2^+$  and  $N^+$  from mixtures of 20%  $N_2$  in argon are shown in Figs. 6(c) and 6(d), respectively. The IEDs for these ions are significantly nar-

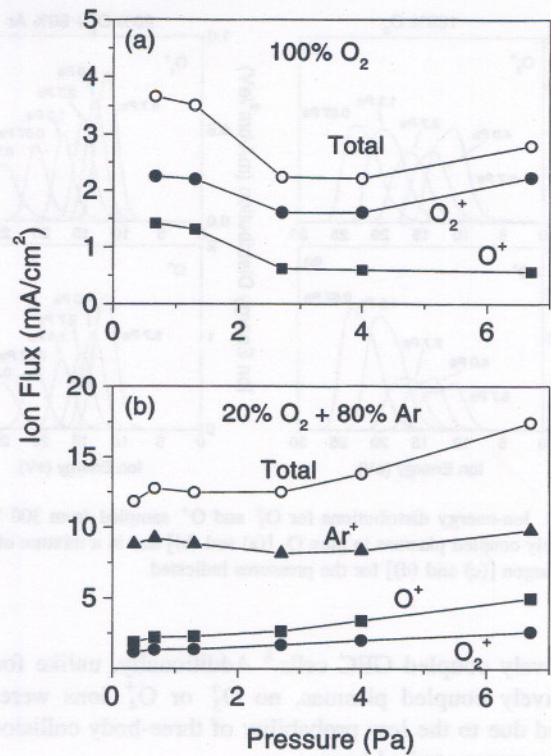


FIG. 7. Absolute ion flux densities at the grounded electrode for 300 W inductively coupled plasmas in (a) pure  $O_2$  and in (b) a mixture (by volume) of 20%  $O_2$  with argon. The open symbols ( $\circ$ ) are the total ion flux densities derived from the total current measurements. The closed symbols are determined from the relative intensities of the measured IEDs for each ion scaled to the total flux densities: ( $\bullet$ )  $O_2^+$ , ( $\blacksquare$ )  $O^+$ , and ( $\blacktriangle$ )  $Ar^+$ .

rower than those measured from pure nitrogen, exhibiting a FWHM only slightly larger than for pure argon. This is consistent with the larger electron (and ion) densities of the argon-containing plasmas, as discussed in the previous paragraph. The mean energies of the IEDs are nearly identical to the plasma potentials shown in Fig. 4 for pure argon.

### C. Oxygen and Ar:O<sub>2</sub> mixtures

Figure 7(a) shows the ion flux densities at the grounded electrode for 300 W inductively coupled plasmas generated in pure oxygen for pressures ranging from 0.34 to 6.7 Pa. The total ion fluxes (shown by open circles) in pure  $O_2$  are comparable to those in pure  $N_2$ , and are significantly less than in pure argon for all pressures. This is consistent with measurements of electron densities showing magnitudes for  $N_2$  and  $O_2$  that are comparable to each other but significantly below measured electron densities in argon.<sup>16</sup> The total ion flux does not present a clear trend as a function of pressure, exhibiting a minimum between 2 and 4 Pa.

The solid symbols in Fig. 7(a) represent the relative contributions of the  $O_2^+$  and  $O^+$  ions to the total ion flux density. Similar to  $N_2^+$ , the  $O_2^+$  ion is the dominant ion at all pressures, with the atomic ion  $O^+$  accounting for between 20% and 40% of the total ion flux. While the  $O_2^+$  flux dominates the total ion signal, the relative magnitude of the  $O^+$  flux compared to the  $O_2^+$  flux with the inductively coupled plasma source is significantly greater than observed in ca-

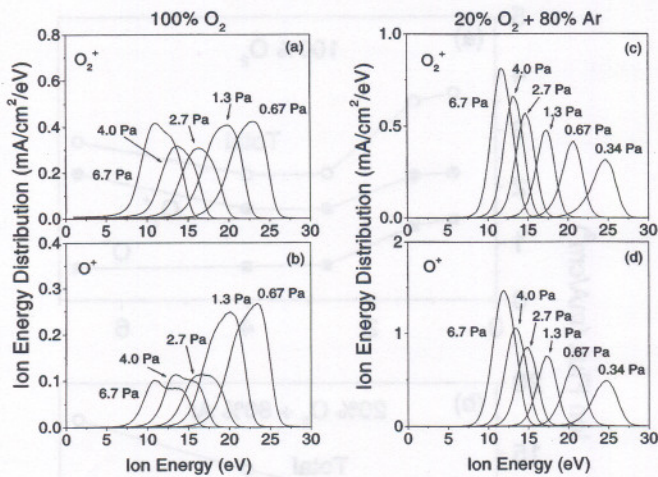


FIG. 8. Ion-energy distributions for O<sub>2</sub><sup>+</sup> and O<sup>+</sup> sampled from 300 W inductively coupled plasmas in pure O<sub>2</sub> [(a) and (b)] and in a mixture of 20% O<sub>2</sub> in argon [(c) and (d)] for the pressures indicated.

capacitively coupled GEC cells.<sup>8</sup> Additionally, unlike for capacitively coupled plasmas, no O<sub>3</sub><sup>+</sup> or O<sub>4</sub><sup>+</sup> ions were observed due to the low probability of three-body collisions at the pressures studied here.

Figure 7(b) shows the total ion flux for an inductively coupled plasma sustained in a 20% O<sub>2</sub>:80% Ar mixture at 300 W as a function of gas pressure. The total flux density is nearly constant at lower pressures, exhibiting a small increase with increasing pressure above 3 Pa. As for the Ar:N<sub>2</sub> mixture, the magnitude of the total ion flux density for the mixture with argon is significantly greater than for the pure molecular gas.

The dominant ion detected from the argon mixture is again Ar<sup>+</sup>. The oxygen ions exhibit significant, but smaller, intensities. In contrast to the Ar:N<sub>2</sub> mixtures, and to the pure oxygen plasmas, O<sup>+</sup> is the dominant ion from the molecule, accounting for nearly twice the ion flux as O<sub>2</sub><sup>+</sup> at all pressures. Reactions with metastable argon, similar to those proposed for nitrogen in the previous section, are expected to exist for oxygen, and may account for the relative increase in O<sup>+</sup> flux with the addition of argon to the oxygen plasma.

The ion-energy distributions for O<sub>2</sub><sup>+</sup> and O<sup>+</sup> from pure O<sub>2</sub> are shown in Figs. 8(a) and 8(b), respectively. The IEDs for O<sub>2</sub><sup>+</sup> and O<sup>+</sup> are similar in shape, and as for N<sub>2</sub>, exhibit nearly the same mean energies. The widths of the IEDs from pure oxygen discharges are broader (FWHM=5.0 eV) than the IEDs for Ar<sup>+</sup> in pure argon, but narrower than observed for IEDs from nitrogen. At the highest pressures the IEDs exhibit some evidence of splitting, with O<sup>+</sup> showing the greatest effect due to its lighter mass. This is consistent with increased capacitive coupling across the ground sheath compared to argon plasmas, as observed in pure N<sub>2</sub> plasmas. The mean energies of the oxygen IEDs are approximately the same as those measured for argon.

The ion-energy distributions for O<sub>2</sub><sup>+</sup> and O<sup>+</sup> from mixtures of 20% O<sub>2</sub> in argon are shown in Figs. 8(c) and 8(d), respectively. The IEDs for these ions are clearly narrower than those measured from pure oxygen, exhibiting a FWHM slightly narrower than for pure argon. Again, the mean ener-

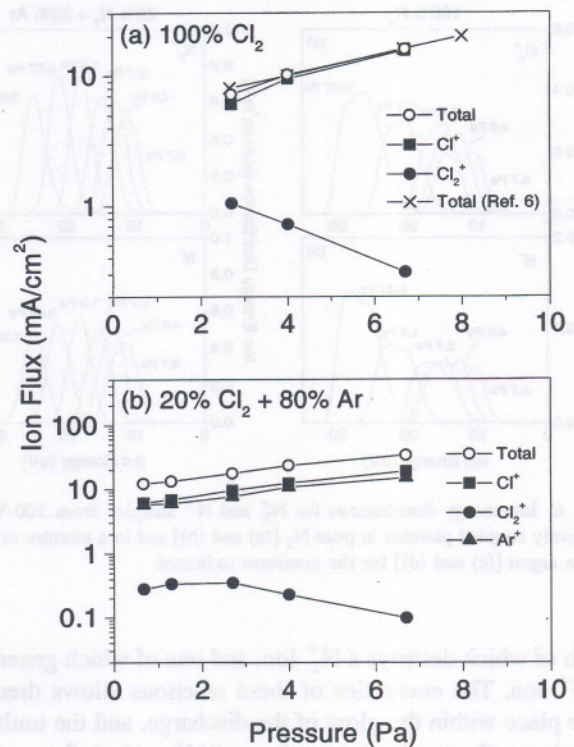


FIG. 9. Absolute ion flux densities at the grounded electrode for 300 W inductively coupled plasmas in (a) pure Cl<sub>2</sub> and in (b) a mixture (by volume) of 20% Cl<sub>2</sub> with argon. The open symbols (○) are the total ion flux densities derived from the total current measurements. The previous data of Woodworth *et al.* (see Ref. 6) are shown for comparison (×). The closed symbols are determined from the relative intensities of the measured IEDs for each ion scaled to the total flux densities: (●) Cl<sub>2</sub><sup>+</sup>, (■) Cl<sup>+</sup>, and (▲) Ar<sup>+</sup>.

gies of the IEDs are nearly identical to the plasma potentials shown in Fig. 4 for pure argon.

### D. Chlorine and Ar:Cl<sub>2</sub> mixtures

Figure 9(a) shows the ion flux densities at the grounded electrode for 300 W inductively coupled plasmas generated in pure chlorine for pressures ranging from 2.7 to 6.7 Pa. The magnitude of the total ion flux (shown by open circles) increases with pressure, and while smaller than pure argon, is significantly greater than measured in pure nitrogen or oxygen. The present measurements are in excellent agreement with previous measurements<sup>6</sup> of total ion flux density in inductively coupled chlorine plasmas in a GEC cell. This consistency may be fortuitous because of the significant changes in surface conditions that are commonly observed in chlorine discharges,<sup>6,19</sup> which make it difficult to ensure that identical conditions exist in two different reactors.

As can be seen in Fig. 9(a), the ion flux consists almost entirely of Cl<sup>+</sup> at all pressures, with almost no contribution from Cl<sub>2</sub><sup>+</sup>. This is the first diatomic molecule investigated here for which the fragment ion flux generated in a discharge of the pure gas exceeds the parent ion flux. Interestingly, Woodworth *et al.*<sup>7</sup> observed nearly equal intensities of Cl<sub>2</sub><sup>+</sup> and Cl<sup>+</sup> ions in a pure chlorine discharge at 200 W, which is

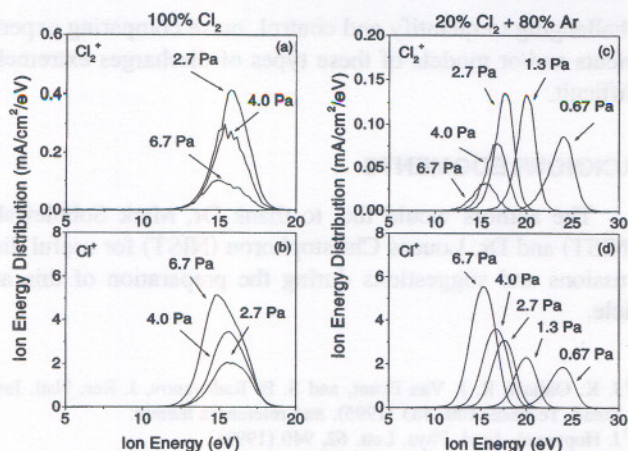


FIG. 10. Ion-energy distributions for  $\text{Cl}_2^+$  and  $\text{Cl}^+$  sampled from 300 W inductively coupled plasmas in pure  $\text{Cl}_2$  [(a) and (b)] and in a mixture of 20%  $\text{Cl}_2$  [(c) and (d)] in argon for the pressures indicated.

in apparent disagreement with the results presented here, and is most likely attributable to differences in surface conditions.

Figure 9(b) shows the total ion flux for an inductively coupled plasma sustained in a 20%  $\text{Cl}_2$ /80% Ar mixture at 300 W as a function of gas pressure. The total flux density increases as a function of pressure, consistent with other measurements made for Ar: $\text{Cl}_2$  mixtures at 200 W,<sup>7</sup> and similar to the measurements made here in mixtures of argon and oxygen. The magnitude of the total ion flux measured here is approximately 30% greater than reported previously<sup>7</sup> at 200 W.

As for the other mixtures, the magnitude of the total ion flux density for the mixture (Ar: $\text{Cl}_2$ ) is greater than for the pure gas (chlorine). However, the difference is smaller in this case than for nitrogen or oxygen. The dominant ion detected from the argon-chlorine mixture is  $\text{Cl}^+$ , in contrast to the other mixtures for which  $\text{Ar}^+$  was clearly the most abundant ion for all plasma conditions studied. The  $\text{Cl}_2^+$  ion accounts for only a very small fraction of the ion flux detected from the Ar: $\text{Cl}_2$  mixture at all pressures, with the relative intensity of the molecular ion again decreasing significantly with the addition of argon to the discharge. The relative intensities of the  $\text{Cl}^+$  and  $\text{Ar}^+$  ions agree well with previous data taken for a 2.67 Pa plasma at 200 W, but the relative intensity of the  $\text{Cl}_2^+$  flux is again significantly below the results of Woodworth and co-workers.<sup>7</sup>

As for nitrogen and oxygen, the decrease in  $\text{Cl}_2^+$  ion intensity when mixed with argon may be attributed to reactions of the ions with metastable argon. Again, all reactions corresponding to those discussed in Sec. III B are energetically allowed for chlorine. One potential difference between chlorine and the other two molecular gases studied here ( $\text{N}_2$  and  $\text{O}_2$ ) is that Penning ionization is energetically possible. However, the effect of Penning ionization is not clear from the present experiments.

The ion-energy distributions for  $\text{Cl}_2^+$  and  $\text{Cl}^+$  from pure  $\text{Cl}_2$  are shown in Figs. 10(a) and 10(b), respectively. The IEDs for  $\text{Cl}_2^+$  and  $\text{Cl}^+$  are similar in shape, each exhibiting some broadening indicative of increased capacitive coupling

compared to argon, with the IEDs for  $\text{Cl}^+$  exhibiting more broadening due to their lesser mass. The previously published IEDs of Woodworth *et al.*<sup>6</sup> in pure chlorine are similar in shape to those shown here, but the values of the mean energies of the IEDs differ by as much as 5 V, with our values being higher.

The ion-energy distributions for  $\text{Cl}_2^+$  and  $\text{Cl}^+$  from mixtures of 20%  $\text{Cl}_2$  in argon at 300 W are shown in Figs. 10(c) and 10(d), respectively. The IEDs for these ions are narrower than those measured from pure chlorine. The mean energies of the IEDs for discharges above 2.7 Pa are similar to those measured in pure chlorine, and in general are several eV higher than the plasma potentials shown in Fig. 4 for pure argon. Agreement with the mean energies presented previously by Woodworth *et al.*<sup>7</sup> is poor, with our values being 5 eV higher at 6.7 Pa increasing to 10 eV higher at 0.67 Pa.

Many models of chlorine-containing plasmas have been published, but a direct comparison with the experimental data is often difficult due to differences in assumed reactor geometries and plasma conditions. However, for models that calculate ion flux densities, a qualitative comparison is useful. Two models by Kushner and co-workers<sup>20,21</sup> of inductively coupled plasmas in Ar: $\text{Cl}_2$  mixtures predict that  $\text{Cl}_2^+$  is the dominant ion, in apparent contradiction with the measurements presented here. A model by Wise, Lymberopoulos and Economou<sup>22</sup> predicts that the dominant ion in a high density, rf, chlorine plasma will depend upon pressure and wall effects, with  $\text{Cl}^+$  generally being the dominant ion at low pressures. Another model by Lymberopoulos and Economou<sup>23</sup> predicts that the  $\text{Cl}^+$  flux in a pure  $\text{Cl}_2$  inductively coupled plasma will exceed the  $\text{Cl}_2^+$  flux by an order of magnitude, similar to that observed here. These disparate results indicate the obvious need to model similar reactor geometries, but also indicates that there may be significant difficulties in modeling  $\text{Cl}_2$  plasmas because of the potential impact of unquantifiable surface conditions.

#### IV. CONCLUSIONS

The results presented here for inductively coupled argon plasmas, including ion energy distributions, mean energies, and absolute ion flux densities, are in general agreement with the previously published results of Woodworth *et al.*<sup>5</sup> obtained on another GEC rf reference cell. This agreement validates both experiments, and provides a measure of the level of agreement that can be expected in these types of measurements on similar reactors.

The ability to mass analyze the ions striking the electrode surface allows a fuller understanding of the composition of the ion flux and of the chemistry and physics occurring within the plasma glow. For plasmas in pure  $\text{N}_2$  the dominant ion was the molecular ion  $\text{N}_2^+$ , with  $\text{N}^+$  contributing about 25% to the total ion flux. For plasmas in a mixture of argon and nitrogen,  $\text{Ar}^+$  was the dominant ion with  $\text{N}_2^+$  and  $\text{N}^+$  exhibiting nearly equal intensities, and accounting for approximately half of the total ion flux. Similar results were observed for the oxygen-containing plasmas, except that  $\text{O}^+$  exhibited a larger flux than  $\text{O}_2^+$  in the plasmas generated in the argon:oxygen mixtures. The ion fluxes mea-

sured for the chlorine-containing plasmas exhibited significantly different behavior with  $\text{Cl}^+$  being the dominant ion for all conditions studied here. The  $\text{Cl}_2^+$  ion flux was as much as an order of magnitude below the  $\text{Cl}^+$  flux in pure  $\text{Cl}_2$  discharges, and exceeded an order of magnitude below  $\text{Cl}^+$  in the mixture with argon.

For all of the molecular gases studied here, the parent ion flux decreased, compared to the atomic ion flux, when argon was added to the pure gas discharge. One possible explanation for this observation is that there is a strong interaction between metastable argon atoms in the discharge and the molecular ions that results in the dissociation (and destruction) of the ion. This type of process is energetically allowed for nitrogen, oxygen, and chlorine, but no fundamental data are available to confirm the likelihood of such reactions.

The mean energies of the ions sampled from mixtures of argon with  $\text{N}_2$ ,  $\text{O}_2$ , and  $\text{Cl}_2$  (which correspond to the plasma potentials of the discharge) were all nearly the same as measured in pure argon, which could indicate that the electron energy distribution is largely determined by the 80% argon in the mixture, and not the 20% molecular gas. However, the mean ion energies measured for the pure gases were also fairly consistent with one another, indicating that the plasma potentials (and therefore mean electron energies) generated in GEC rf reference cells are primarily dependent upon pressure and not gas composition or power.

Total ion fluxes varied considerably with power, gas composition, and pressure. At 300 W, the largest observed ion fluxes were from the argon plasmas, and the smallest were from the  $\text{N}_2$  and  $\text{O}_2$  plasmas. The ion fluxes from the mixtures were fairly consistent in magnitude with the pure argon plasmas, and the ion fluxes from the pure  $\text{Cl}_2$  plasma were significantly larger than those measured from pure  $\text{O}_2$  or  $\text{N}_2$ .

While reasonable agreement was obtained between the present measurements and those previously published by Woodworth *et al.*<sup>5</sup> for argon plasmas, significant differences were observed in mean ion energies and relative ion intensities from the chlorine-containing plasmas.<sup>6,7</sup> Absolute total ion flux densities, however, were in reasonable agreement. It is likely that these large discrepancies are due to the observed differences in the surface conditions that result from the running of chlorine discharges. These changes, which are

challenging to quantify and control, make comparing experiments and/or models of these types of discharges extremely difficult.

## ACKNOWLEDGMENTS

The authors would like to thank Dr. Mark Sobolewski (NIST) and Dr. Loucas Christophorou (NIST) for useful discussions and suggestions during the preparation of this article.

- <sup>1</sup>J. K. Olthoff, R. J. Van Brunt, and S. B. Radovanov, *J. Res. Natl. Inst. Stand. Technol.* **100**, 383 (1995), and references therein.
- <sup>2</sup>J. Hopwood, *Appl. Phys. Lett.* **62**, 940 (1993).
- <sup>3</sup>U. Kortshagen and M. Zethoff, *Plasma Sources Sci. Technol.* **4**, 541 (1995).
- <sup>4</sup>G. Mümken and U. Kortshagen, *J. Appl. Phys.* **80**, 6639 (1996).
- <sup>5</sup>J. R. Woodworth, M. E. Riley, D. C. Meister, B. P. Aragon, M. S. Le, and H. H. Sawin, *J. Appl. Phys.* **80**, 1304 (1996).
- <sup>6</sup>J. R. Woodworth, M. E. Riley, P. A. Miller, G. A. Hebner, and T. W. Hamilton, *J. Appl. Phys.* **81**, 5950 (1997).
- <sup>7</sup>J. R. Woodworth, M. E. Riley, P. A. Miller, C. A. Nichols, and T. W. Hamilton, *J. Vac. Sci. Technol. A* **15**, 3015 (1997).
- <sup>8</sup>R. J. Van Brunt, J. K. Olthoff, and S. B. Radovanov, *Proceedings of the Eleventh International Conference on Gas Discharges and Their Applications* (Chuo University, Tokyo, Japan, 1995), pp. I486–I489.
- <sup>9</sup>P. J. Hargis *et al.*, *Rev. Sci. Instrum.* **65**, 140 (1994).
- <sup>10</sup>J. K. Olthoff and K. E. Greenberg, *J. Res. Natl. Inst. Stand. Technol.* **100**, 327 (1995).
- <sup>11</sup>P. A. Miller, G. A. Hebner, K. E. Greenberg, P. S. Pochan, and B. P. Aragon, *J. Res. Natl. Inst. Stand. Technol.* **100**, 427 (1995).
- <sup>12</sup>J. K. Olthoff, R. J. Van Brunt, S. B. Radovanov, J. A. Rees, and R. Surowiec, *J. Appl. Phys.* **75**, 115 (1994).
- <sup>13</sup>M. V. V. S. Rao, R. J. Van Brunt, and J. K. Olthoff, *Phys. Rev. E* **54**, 5641 (1996).
- <sup>14</sup>NIST/EPA/NIH Mass Spectral Database, PC Version 4.5, NIST Standard Reference Database 1A (February 1994).
- <sup>15</sup>M. A. Sobolewski, *Appl. Phys. Lett.* **72**, 1146 (1998).
- <sup>16</sup>A. Schwabedissen, E. C. Benck, and J. R. Roberts, *Phys. Rev. E* **55**, 3450 (1997).
- <sup>17</sup>R. W. Molof, H. L. Schwartz, T. M. Miller, and B. Bederson, *Phys. Rev. A* **10**, 1131 (1974).
- <sup>18</sup>L. G. Christophorou and I. Illenberger, *Phys. Lett. A* **173**, 78 (1993).
- <sup>19</sup>Y. Wang, R. J. Van Brunt, and J. K. Olthoff, *J. Appl. Phys.* **83**, 703 (1998).
- <sup>20</sup>P. L. G. Ventzek, M. Grapperhaus, and M. J. Kushner, *J. Vac. Sci. Technol. B* **12**, 3118 (1994).
- <sup>21</sup>R. J. Hoekstra and M. J. Kushner, *J. Appl. Phys.* **79**, 2275 (1996).
- <sup>22</sup>R. S. Wise, D. P. Lymberopoulos, and D. J. Economou, *Plasma Sources Sci. Technol.* **4**, 317 (1995).
- <sup>23</sup>D. P. Lymberopoulos and D. J. Economou, *IEEE Trans. Plasma Sci.* **23**, 573 (1995).